nature climate change

Article

https://doi.org/10.1038/s41558-024-02147-3

# Arctic soil carbon trajectories shaped by plant–microbe interactions

Received: 14 June 2023

Accepted: 30 August 2024

Published online: 03 October 2024

Check for updates

Megan B. Machmuller[1], Laurel M. Lynch[2], Samantha L. Mosier[1], Gaius R. Shaver[3], Francisco Calderon[4], Laura Gough[5], Michelle L. Haddix[1], Jennie R. McLaren[6], Eldor A. Paul[7], Michael N. Weintraub[8], M. Francesca Cotrufo[1] & Matthew D. Wallenstein[1]

Rapid warming in the Arctic threatens to amplify climate change by releasing the region's vast stocks of soil carbon to the atmosphere. Increased nutrient availability may exacerbate soil carbon losses by stimulating microbial decomposition or offset them by increasing primary productivity. The outcome of these competing feedbacks remains unclear. Here we present results from a long-term nutrient addition experiment in northern Alaska, United States, coupled with a mechanistic isotope-tracing experiment. We found that soil carbon losses observed during the first 20 years of fertilization were caused by microbial priming and were completely reversed in the subsequent 15 years by shrub expansion which promoted an increasingly efficient carbon–nitrogen economy. Incorporating long-term stoichiometric responses in Earth system models will improve predictions of the magnitude, direction and timing of the Arctic carbon–climate feedback.

Arctic soils alone store twice as much carbon (C) as the entire atmosphere[1]. However, this critical terrestrial C stock is increasingly vulnerable as high-latitude ecosystems continue warming much faster (up to four times more) than the global average[2]. As temperature constraints on biological processes lessen[3], soil organic C (SOC) losses from accelerated microbial decomposition may outpace C gains from enhanced plant productivity, driving considerable net C losses to the atmosphere[4–7]. The direction and magnitude of changes in the Arctic C cycle also hinge on complex biological responses to shifts in element concentrations[8]. Carbon cycling in Arctic soils and vegetation is strongly nitrogen (N) limited[9,10], which can constrain rates of primary productivity (C inputs) and microbial decomposition (SOC losses)[7,11–13]. Interactions among these processes could induce positive priming, where new plant inputs fuel microbial processing of soil organic matter (SOM) to acquire N, reducing SOC storage even further[6,14–16]. Alternatively, as plant communities shift from graminoid- to shrub-dominated tundra[17], associated changes in nutrient availability could boost the efficiency of microbial metabolism and SOC accrual[18]. The degree to which changes in plant community composition and N availability influence SOC storage will therefore depend on how shifts in the quantity and quality of plant litter inputs and root exudates[19,20] influence microbial metabolic efficiency[18]. Because graminoids and shrubs differ in their N acquisition strategies, phenological traits and mycorrhizal association[21–23], shrub expansion could modulate C–climate feedbacks.

Given complex interactions across the plant–soil–microbe continuum, it is challenging to constrain modelled projections of the Arctic C balance. Models consistently predict increases in net primary productivity (NPP) due to warming but the effects on SOC, which is a much larger and more persistent C pool, range from substantial losses to substantial gains[24–26]. Uncertainty may arise from inaccurately representing SOC dynamics, as model representation of SOC responses to climate change often conflict with our emerging understanding of SOC formation and persistence[27]. Long-term field experiments and observations that capture coupled C–nutrient dynamics and ecosystem

[1]Department of Soil and Crop Science, Colorado State University, Fort Collins, CO, USA. [2]Department of Soil and Water Systems, University of Idaho, Moscow, ID, USA. [3]The Ecosystems Center, Marine Biological Laboratory, Woods Hole, MA, USA. [4]Columbia Basin Agricultural Research Center, Oregon State University, Adams, OR, USA. [5]Department of Biological Sciences, Towson University, Towson, MD, USA. [6]Department of Biological Sciences, University of Texas, El Paso, TX, USA. [7]Natural Resource Ecology Laboratory, Colorado State University, Fort Collins, CO, USA. [8]Department of Environmental Sciences, University of Toledo, Toledo, OH, USA. e-mail: megan.machmuller@colostate.edu

https://doi.org/10.1038/s41558-024-02147-3

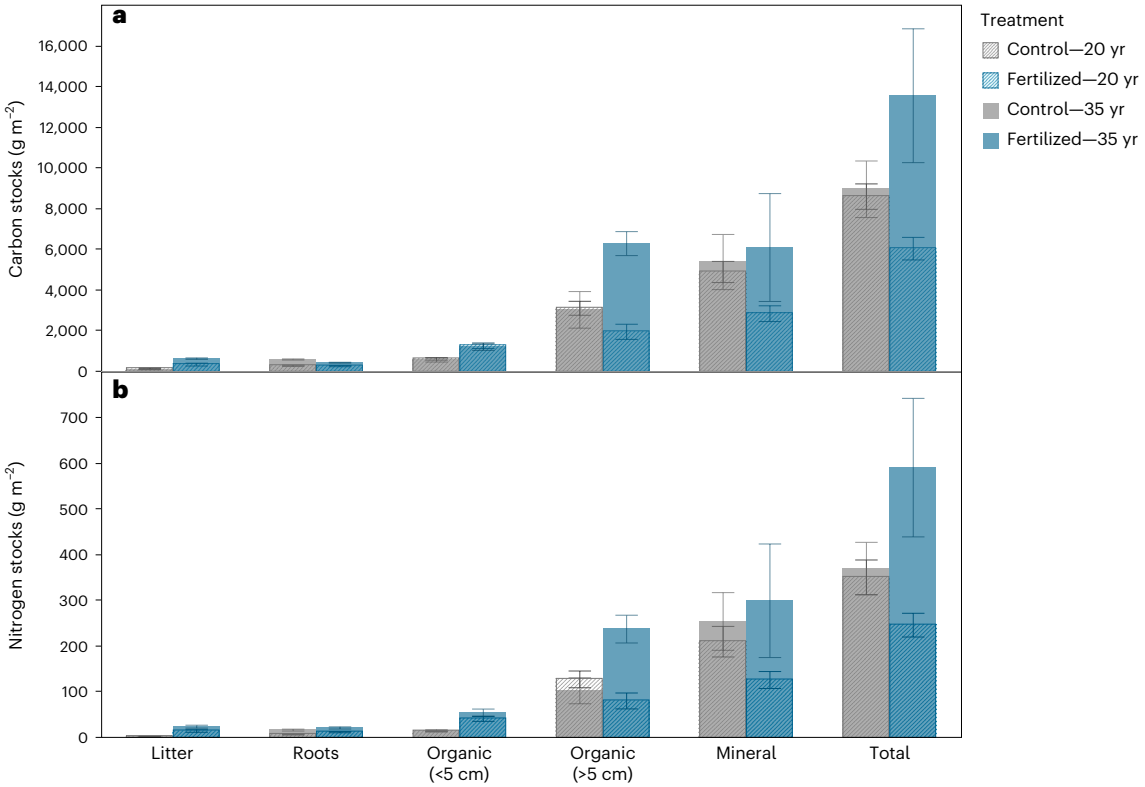


**Fig. 1 | Transient effect of fertilization on soil C and N stocks. a**,**b**, Soil C (**a**) and N (**b**) stock comparisons after 20 yr (ref. 7) and 35 yr of continuous fertilization. Soil organic and mineral stocks exclude roots. Bars represent block means ± s.e. ($n$ = 4); significant differences between treatments shown in Fig. 2. Please note that greater thawed thickness accounted for deeper sampling of mineral soil layers in the 35th year compared to the 20th year (by ~4 cm in control and ~6 cm in fertilized plots).

structural changes are therefore critical to evaluate model performance and improve model projections[28].

Here, we present data from a 35 yr fertilization experiment in moist acidic tundra (MAT)[21] at the Arctic Long-Term Ecological Research site near Toolik Lake, Alaska, United States (68° 38′ N, 149° 34′ W). Established in 1981, the field experiment was originally designed to test the response of Arctic tundra vegetation to chronic press disturbances (for example, N and P fertilization, passive warming, changes in light availability)[22]. We resampled experimental plots (split-block design consisting of 5 × 20 m$^2$ fertilized and unfertilized plots in four replicate blocks with 1 m buffer strips) which were continuously fertilized since 1981 (10 gN and 5 gP m$^{-2}$ yr$^{-1}$). After 20 years (see results from ref. 7) and 35 years (this study) of fertilization, C and N stocks within the seasonally thawed active layer were quantified for the following pools: litter (leaf and wood), roots, upper organic soil layer (0–5 cm), lower organic soil layer (>5 cm) and mineral soil layer (~17–27 cm; Methods). It was previously found that 20 years of fertilization dramatically altered plant species composition and reduced SOC stocks by nearly 2,000 gC m$^{-2}$ (~20% of total active layer SOC), despite nearly doubling aboveground productivity[7]. These initial results supported a long-held paradigm that the Arctic will become a net C source under future climate scenarios[7]. We resampled the same plots 15 years later to: (1) evaluate whether the trajectory of long-term SOC loss changed between the 20th and 35th years of experimental fertilization; and (2) systematically explore how the observed transition from graminoid- to shrub-dominated tundra[17] influenced microbial metabolism, SOM chemistry and SOC stocks[18].

## Long-term experiment reveals new soil C trajectories

Countering previous findings, we show that the SOC trajectory changed from loss to gain between the 20th and 35th years of experimental fertilization. Within this 15 yr period, SOC stocks in fertilized plots recovered to, or even exceeded, those in control plots (Fig. 1a). Although the first 20 years of fertilization reduced C and N stocks in the lower organic and mineral soil layers, this effect disappeared after 35 years in the mineral layer and reversed in the lower organic layer, where SOC and N stocks were on average twice as high as control stocks ($P$ < 0.05, Fig. 1). Consistent with findings after 20 years, experimental fertilization increased SOC and N stocks in the litter layer ($P$ < 0.01) and upper organic ($P$ < 0.01) soil layers (Fig. 1) but increases within these pools were often greater after 35 years (Fig. 2). Our findings underscore the potential for complex feedbacks to emerge across decades that produce nonlinear responses and potential state changes among ecosystem components[28–30].

Weather and climate factors alone cannot explain these unexpected and transient SOC dynamics. In the 35th year of fertilization, we detected no change in total thaw layer thickness between control (27.1 ± 2.35 cm) and fertilized (25.4 ± 1.1 cm) plots (Supplementary Table 1), suggesting that increases in SOC stocks were not driven by deeper thaw depth due to fertilizer treatment alone. While the bulk density of organic soil layers was significantly higher in fertilized than in control plots in both the 20th and 35th year of experimentation (Supplementary Table 1), we observed no fertilizer effect on mineral layer bulk density in either year (0.66 g cm$^{-3}$ in the 20th year of experimentation and 1.2 g cm$^{-3}$ in the 35th year of experimentation). The apparent change in mineral layer bulk density between years was due entirely to the greater thawed thickness of the mineral layer in the 35th year of experimentation (by ~4 cm in control and ~6 cm in fertilized plots). Reflecting general trends in soil properties with depth[31,32], the thicker mineral layer in the 35th year of experimentation had a lower SOC concentration and higher bulk density than the shallower mineral layer sampled 15 years before. While changes in bulk density with ongoing

https://doi.org/10.1038/s41558-024-02147-3

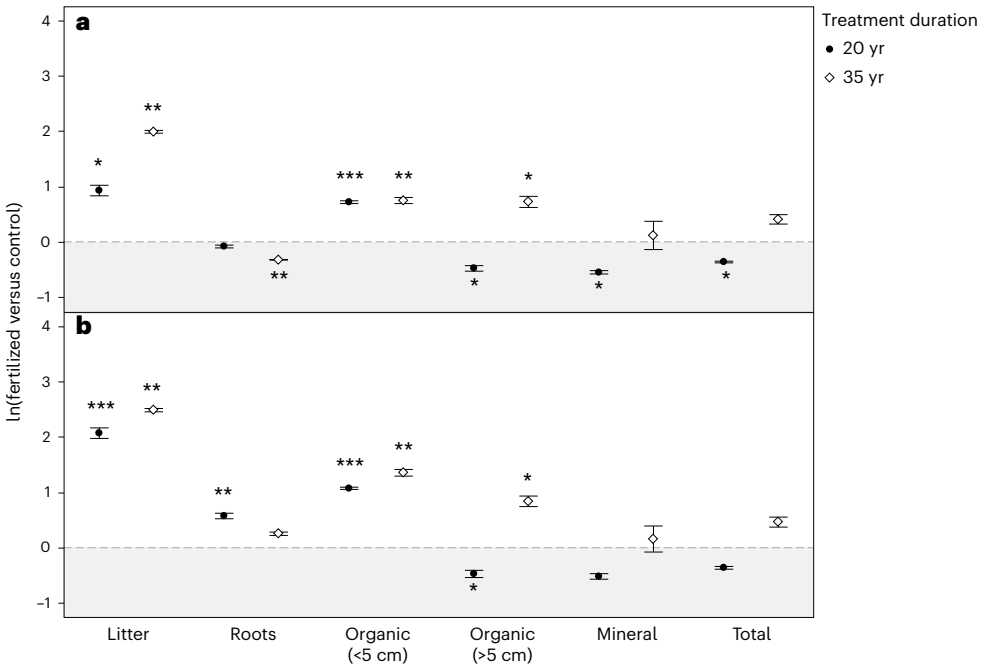


**Fig. 2 | Fertilization effect size on soil C and N stocks.** Log response ratios of litter, root and soil C and N stocks (g m$^{-2}$) after 20 and 35 yr of fertilization. **a**,**b**, Belowground C (**a**) and N (**b**) stocks include roots, litter (wood, leaf and loose) and soil (excluding roots), where values represent the mean ($n$ = 4) and standard error of the natural log ratio of fertilized versus control stocks. Ratios >0 indicate that stocks were greater in fertilized plots than in control plots and vice versa for ratios <0 (shaded). Accordingly, asterisks denote results of two-sided Tukey's HSD tests between field treatments (fertilized versus control) within each sampling year (for example, 20th or 35th year of experimentation), adjusted for multiple comparisons; *$P$ < 0.05, **$P$ < 0.01 or ***$P$ < 0.001.

permafrost degradation are understudied, bulk density can be sensitive to changes in environmental conditions[32] and should be monitored to accurately predict changes in Arctic SOC storage under novel climate[33]. Nevertheless, even after accounting for long-term changes in soil properties (for example, bulk density, pH and soil moisture content), the significant net loss of SOC observed after 20 years of experimentation is no longer apparent after 35 years (Fig. 2). These trends can only be driven by net SOC accrual in fertilized plots, as SOC stocks in control plots did not change. As we observed no evidence of recent cryoturbation, physical mechanisms alone cannot fully explain the observed change of direction in SOC dynamics (that is, from SOC loss to net SOC accrual, Fig. 2), leading us to examine changes in biological function.

## Fertilization-induced changes in plant community composition

Fertilization significantly reduced plant community diversity, resulting in almost complete replacement of the dominant moss, graminoid and evergreen species (*Eriophorum vaginatum, Sphagnum* spp., *Hylocomium splendens, Vaccinium vitis-idaea* and *Rhododendron tomentosum*)[22] by deciduous shrubs (*Betula nana*, 90% cover)[34]. Widespread increases in deciduous shrub abundance have been observed across high-latitude systems[17,35,36], including within our control plots (for example, the relative abundance of *B. nana* biomass gradually increased from ~25% to ~32% between the 20th and 35th year of fertilization, G.R.S. unpublished data). In fertilized plots, *B. nana* biomass increased by 43% (667 ± 143 to 955 ± 170 g m$^{-2}$), *E. vaginatum* biomass declined by 21% (121 ± 17 to 95 ± 38 g m$^{-2}$) and total NPP (including above and belowground production) inputs were ~11,000 gC m$^{-2}$ between 2000 and 2015. During this same period, average NPP inputs in control plots were ~9,000 gC m$^{-2}$ and we observed minimal change in SOC (+943 ± 1,520 g m$^{-2}$) and soil N (+36 ± 67 gN m$^{-2}$) (Fig. 1; Methods). These trends suggest that current rates of shrub expansion create a tightly coupled C–N economy, building up SOC through a positive feedback loop (for example, on average, 64% of NPP is retained in fertilized plots versus ~10% in control plots). Similar patterns have been observed in low Arctic systems following shrub expansion (for example, gains of 29 ± 9 gC m$^{-2}$ yr$^{-1}$) (ref. 37). Within control plots, increases in soil N could be caused via four potential mechanisms: greater permafrost thaw depths (which we did not observe), atmospheric N deposition, N fixation (trends did not change between 1984 and 2016)[38] or SOM turnover. Upper estimates on atmospheric N deposition (0.2–0.3 gN m$^{-2}$ yr$^{-1}$) (ref. 39) and N fixation (0.08–0.13 gN m$^{-2}$ yr$^{-1}$) (ref. 40) can account for up to 20% of the observed increase in soil N (36 gN per m$^2$ in 15 years), suggesting increases in SOM turnover (for example, via changes in plant inputs or microbial decomposition) as the predominant mechanism.

Shrub expansion is facilitated by phenotypic plasticity and other physiological traits that allow them to outcompete other species under warmer temperatures[41] and greater N availability[7,34,42]. The loss of graminoids from the fertilized plots, in particular, reduced inputs of polysaccharide-rich, high C:N leaf litter (~48 for *E. vaginatum*) and increased inputs of structurally complex, low C:N *B. nana* leaf litter (~27) (ref. 43) (Supplementary Figs. 1 and 2 and Supplementary Table 4). Shifts in litter input quality (Supplementary Fig. 2c and Supplementary Table 3) cascaded belowground (Supplementary Table 3), increasing the relative abundance of alkyl aromatic and amide moieties and reducing the relative abundance of carbohydrates (Supplementary Figs. 1 and 2a,b) and soil C:N (Table 1). During this same period, total root biomass C stocks declined by 30% ($P$ < 0.01, Fig. 2) and root distribution shifted upwards into surface soil layers. These findings are consistent with the expectation that plants allocate proportionally less biomass belowground as nutrient availability increases[34,44,45] and with the transition from annual, deeply rooted *E. vaginatum* and other graminoids to the longer-lived, shallow roots of *B. nana*[46]. Furthermore, declines in graminoid root mass and presumably dead root accumulation, at depth accounted for up to 40% of the SOC lost in the first 20 years of fertilization[46]. While the slower turnover[47] and decomposition rates[19] of *B. nana* roots could lead to belowground C gains as plant communities shift towards shrub dominance, root C stocks account for only a

https://doi.org/10.1038/s41558-024-02147-3

**Table 1 | Soil biogeochemical attributes in laboratory incubation and field experiment**

| Data source | Soil layer | Field treatment | Laboratory treatment | MB-C(μg per g of soil) | MB-N(μg per g of soil) | DOC(μg per g of soil) | TDN(μg per g of soil) | Soil C:N |
|---|---|---|---|---|---|---|---|---|
| Field experiment | Organic (0–5 cm) | Control | – | 4,881.62 (212.48)$^{A}$ | 489.98 (40.44)$^{A}$ | 880.89 (68.53)$^{A}$ | 56.13 (9.13)$^{BC}$ | 27.53 (2.59)$^{A}$ |
| | | Fertilized | | 2,060.64 (213.87)$^{A}$ | 452.26 (52.33)$^{A}$ | 646.63 (129.14)$^{AB}$ | 634.79 (159.27)$^{A}$ | 20.11 (1.52)$^{B}$ |
| | Organic (>5 cm) | Control | – | 2,878.05 (599.83)$^{A}$ | 359.54 (87.06)$^{AB}$ | 649.81 (53.69)$^{AB}$ | 60.51 (7.08)$^{BC}$ | 28.40 (1.25)$^{A}$ |
| | | Fertilized | | 1,159.35 (244.81)$^{A}$ | 220.05 (37.57)$^{BC}$ | 474.13 (42.26)$^{BC}$ | 194.84 (22.52)$^{AB}$ | 26.64 (1.63)$^{AB}$ |
| | Mineral | Control | – | 230.29 (105.70)$^{AB}$ | 222.69 (9.32)$^{C}$ | 123.41 (19.63)$^{C}$ | 15.60 (2.45)$^{C}$ | 21.66 (0.41)$^{AB}$ |
| | | Fertilized | | 116.16 (56.69)$^{B}$ | 10.76 (5.55)$^{C}$ | 206.48 (126.69)$^{C}$ | 117.21 (99.04)$^{BC}$ | 20.13 (0.59)$^{B}$ |
| SL | | | | *** | *** | *** | *** | *** |
| FT | | | | * | | | *** | ** |
| SL×FT | | | | | | | | |
| Laboratory incubation | Organic | Unfertilized *B. nana* | Control | 2,959.22 (200.78)$^{AB}$ | 377.20 (30.13)$^{ABCD}$ | 917.45 (74.49)$^{B}$ | 34.49 (2.14)$^{C}$ | 34.33 (0.63)$^{BC}$ |
| | | | C | 2,988.77 (287.84)$^{AB}$ | 343.23 (35.15)$^{BCD}$ | 790.15 (61.93)$^{BC}$ | 29.87 (1.37)$^{C}$ | 36.96 (1.43)$^{BC}$ |
| | | | C+N | 3,483.45 (255.43)$^{AB}$ | 942.02 (241.38)$^{AB}$ | 1,225.69 (82.45)$^{A}$ | 1,105.15 (79.17)$^{A}$ | 31.24 (0.61)$^{C}$ |
| | Organic | Unfertilized *E. vaginatum* | Control | 2,295.68 (231.46)$^{B}$ | 259.82 (20.62)$^{D}$ | 541.50 (39.00)$^{CD}$ | 26.75 (2.53)$^{C}$ | 61.25 (3.71)$^{A}$ |
| | | | C | 2,674.49 (361.79)$^{B}$ | 280.08 (28.78)$^{CD}$ | 455.74 (55.95)$^{D}$ | 16.97 (2.18)$^{C}$ | 65.39 (8.09)$^{A}$ |
| | | | C+N | 3,253.70 (185.82)$^{B}$ | 951.25 (207.67)$^{A}$ | 613.51 (30.90)$^{CD}$ | 833.41 (89.04)$^{AB}$ | 43.78 (0.99)$^{B}$ |
| | Organic | Unfertilized mixture | Control | 4,104.81 (248.59)$^{A}$ | 692.36 (123.19)$^{ABC}$ | 705.50 (39.55)$^{BCD}$ | 70.93 (51.97)$^{C}$ | 44.35 (2.43)$^{B}$ |
| | | | C | 3,744.79 (177.67)$^{A}$ | 480.79 (51.07)$^{ABCD}$ | 568.45 (54.50)$^{CD}$ | 86.61 (54.56)$^{C}$ | 37.14 (2.66)$^{BC}$ |
| | | | C+N | 3,340.00 (343.39)$^{A}$ | 580.58 (86.55)$^{ABCD}$ | 820.70 (96.79)$^{BC}$ | 392.81 (85.09)$^{BC}$ | 32.66 (2.92)$^{BC}$ |
| | Organic | Fertilized *B. nana* | Control | 1,254.86 (438.01)$^{C}$ | 311.30 (86.57)$^{BCD}$ | 525.28 (28.38)$^{CD}$ | 863.43 (238.72)$^{AB}$ | 19.92 (1.20)$^{D}$ |
| | | | C | 1,626.35 (214.81)$^{C}$ | 282.78 (68.79)$^{CD}$ | 512.55 (26.88)$^{CD}$ | 874.55 (252.50)$^{AB}$ | 20.61 (1.10)$^{D}$ |
| | | | C+N | 1,091.17 (466.91)$^{C}$ | 381.24 (120.10)$^{ABCD}$ | 515.91 (16.34)$^{CD}$ | 1,294.56 (241.17)$^{A}$ | 20.35 (0.58)$^{D}$ |
| FT | | | | *** | ** | *** | *** | *** |
| LT | | | | | ** | *** | *** | *** |
| FT×LT | | | | | * | * | *** | * |

Measurements after 35-yr-fertilized field plots (upper) and 25 d laboratory incubation. Values from field experiment represent block averages (±s.e.; $n$=4). Soil measurements include MB-C, MB-N, DOC, TDN and soil C:N. Soil nutrient and MB extracts were performed with 0.05 M $K_2SO_4$ for laboratory incubation soils, as opposed to 0.5 M $K_2SO_4$ used for field experiment soils because of the requirements of a weaker salt solution needed for isotopic analysis. Values represent the mean (±s.e.) from laboratory treatment additions of water (control), $^{13}$C-glucose (C) and $^{13}$C-glucose and $NH_4NO_3$ (C+N) to non-fertilized soils underlying *B. nana* ($n$=5), *E. vaginatum* ($n$=5), a non-specific (mixture) of vegetation ($n$=4) and 35-yr-fertilization soils underlying *B. nana* ($n$=3). Treatment means that share the same letter (A–D) are not statistically different from each other. The level of significance from the two-way ANOVA model including soil layer (SL) and field treatment (FT) or laboratory treatment (LT) and their interaction (SL×FT or FT×LT) is reported as *$P$<0.05, **$P$<0.01 or ***$P$<0.001.

small fraction of total belowground C (3% in fertilized plots and 6% in control plots) (Fig. 1) and cannot explain the substantial SOC accrual observed between the 20th and 35th year.

## Laboratory experiments elucidate drivers of soil C dynamics

To reconcile the shift in plant community composition with microbial drivers of SOC cycling, we used a $^{13}$C isotope-tracing laboratory experiment to characterize microbial C use efficiency (CUE)[48] and the susceptibility of SOC stocks to priming (Methods). We collected organic layer soils from previously unfertilized control plots beneath individual shrub (*B. nana*) and graminoid tussock (*E. vaginatum*) plants and within the inter-tussock zone (mixed plant community, with representative MAT species[22]). We also sampled soils in long-term fertilized plots, which were dominated by *B. nana* shrubs for >20 years. For each soil type we simulated fresh plant inputs by adding 10 mgC (~700 μgC per g of dry soil, 0.2% of total soil C) of 10 at% $^{13}$C-glucose C and matched experimental fertilization rates by adding 8.75 mgN (~645 μgN per g of soil, 6% of total soil N) as ammonium nitrate. We selected a low C amendment rate to minimize impacts to ongoing

https://doi.org/10.1038/s41558-024-02147-3

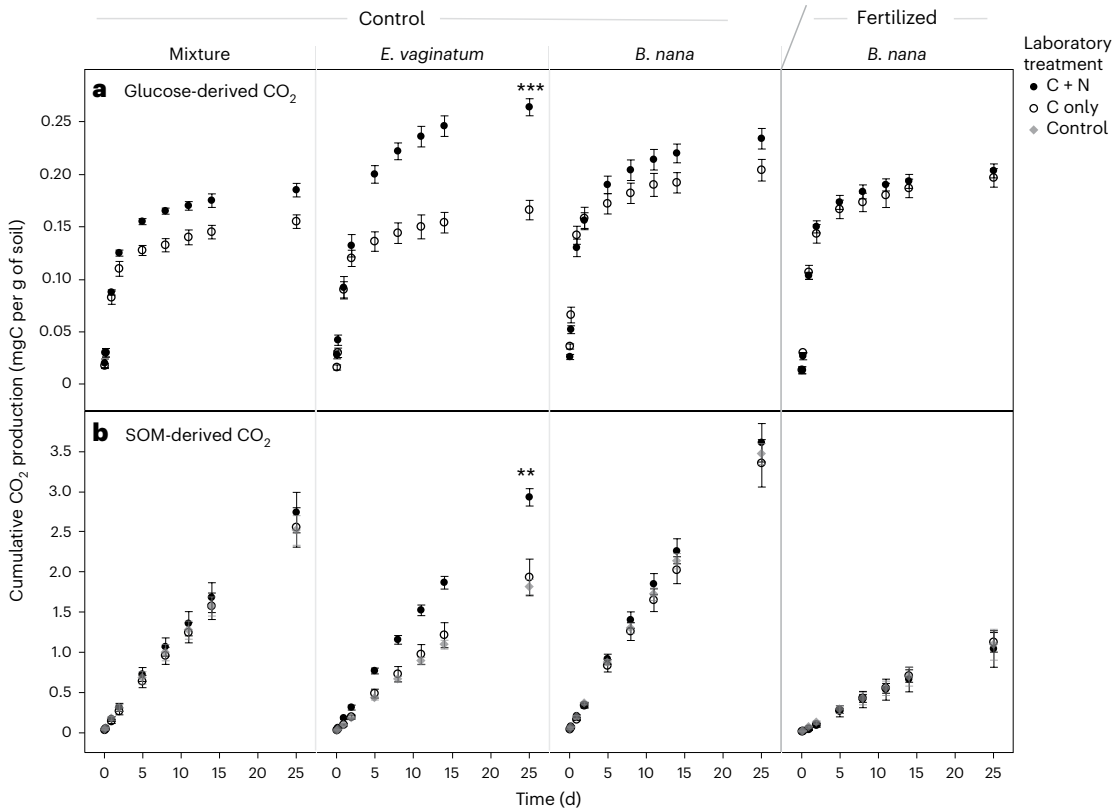


**Fig. 3 | Influence of vegetation and fertilization on microbial substrate use.** **a**,**b**, Cumulative respiration (mgC per g of soil) derived from glucose (**a**) and SOM (**b**) from control soils underlying a non-specific (mixture) of vegetation ($n = 4$), *E. vaginatum* ($n = 5$), *B. nana* ($n = 5$) and 35-yr-fertilization soils underlying *B. nana* ($n = 3$). Treatment additions of glucose C alone (C only, open circles), glucose C and ammonium nitrate (C + N, closed circles) and water (control, diamonds). Points represent means ± s.e. Asterisks denote results of two-sided Tukey's HSD tests of the cumulative flux between treatment additions within each vegetation type, adjusted for multiple comparisons; *$P < 0.05$, **$P < 0.01$ or ***$P < 0.001$.

metabolic processes[49], which we substantiated in our previous field $^{13}$C-tracer experiment[18]. While Arctic microbial communities may be co-limited by N and P (ref. 50), pools of exchangeable and easily weatherable P are typically lower in surface permafrost than are seasonally thawed layers; permafrost thaw would have to increase by >10 cm at our field site before weathering sufficiently increased plant and microbial access to endogenous P (ref. 51). We therefore focus on N availability as a primary driver of observed SOC trajectories. We quantified microbial use of easily assimilable C ($^{13}$C-enriched glucose) versus native SOC by measuring $^{13}$C-$CO_2$ efflux over 25 days and applying mass balance and two-pool mixing models (Methods). We predicted that new C inputs would stimulate the loss of native SOC across all treatments but that we would observe the greatest priming effects in the most N-limited soils (previously unfertilized graminoid soils[18]; Supplementary Table 4).

On the basis of our laboratory incubation results, vegetation composition (shrub, graminoid and mixed community) and soil nutrient status influenced the amount and source (glucose versus native) of C lost via microbial respiration. In the laboratory experiment, adding N to previously unfertilized shrub or mixed community soils did not affect C pools and fluxes (Fig. 3, Supplementary Fig. 3 and Table 2). However, adding N to previously unfertilized, nutrient-deficient graminoid soils, strongly altered C cycling, mimicking trends observed during the first 20 years of field fertilization. Specifically, we found that amending unfertilized graminoid soils with N increased microbial respiration of glucose ($P < 0.0001$, Fig. 3a) and native SOC ($P < 0.001$, Fig. 3b) and decreased the formation of new SOC (Table 2, $P < 0.05$). Dual C and N additions to these graminoid soils also induced a significant positive priming effect, enhancing the loss of native SOC by 73% (Fig. 3). Microbial biomass N (MB-N) increased ($P < 0.01$) without changing microbial biomass C (MB-C) or the CUE of added glucose (Table 2). Overall, we observed SOC priming only in the most N-limited graminoid soils and only when exogenous N was added.

We observed no priming response in soils that had been fertilized for 35 years. Instead, long-term fertilization reduced SOM-derived respiration relative to all previously unfertilized soils ($P < 0.0001$, Fig. 3b). Water-only control respiration in long-term fertilization plots was 60%, 43% and 75% lower than previously unfertilized graminoid, mixed community and shrub soils, respectively. Relative to previously unfertilized shrub soils, long-term fertilization reduced MB-C by 57% and soil dissolved organic C (DOC) concentrations by 43% (Table 1, water-only control). Although microbial communities inhabiting long-term fertilization plots had lower SOM respiration and biomass, they respired proportionately more glucose-derived C when it was available ($P < 0.0001$, Fig. 3), suggesting that they were C limited. Microbial use of new C inputs in shrub-conditioned soils did not induce a positive priming effect, stimulate investment in biomass production or destabilize existing SOC stocks. Our results suggest that greater N availability reduced shrub reliance on microbial communities for nutrient provisioning[52] and the input of structurally complex shrub litter reduced access to easily assimilable C sources, slowing microbial activity and rates of SOC loss.

## Stoichiometric linkages regulate net ecosystem C balance

Here, we highlight how shifts in plant community composition govern microbial energy and nutrient demand[13], ultimately structuring rates of SOC turnover and accumulation. We have previously shown that microbial respiration and belowground retention of low-molecular-weight C

**Table 2 | Measurements after 25 d laboratory incubation from control and fertilized organic soils sampled underneath different vegetation types**

| Field treatment | Laboratory treatment | $^{13C}$MB-C(μg per g of soil) | $^{13C}$DOC(μg per g of soil) | $^{13C}$Soil(μg per g of soil) | $^{13C}CO_2$(mg per g of soil) | CUE[a] | CSE[b] |
|---|---|---|---|---|---|---|---|
| Unfertilized *B. nana* | C | $147.81\pm11.87^{A}$ | $0.87\pm0.13^{A}$ | $343.26\pm52.44^{C}$ | $205.02\pm10.83^{BC}$ | $0.42\pm0.03^{A}$ | $0.61\pm0.05^{B}$ |
| | C+N | $97.68\pm6.31^{ABC}$ | $1.11\pm0.19^{A}$ | $416.73\pm60.52^{BC}$ | $233.88\pm9.30^{AB}$ | $0.34\pm0.04^{A}$ | $0.63\pm0.04^{B}$ |
| Unfertilized *E. vaginatum* | C | $75.33\pm15.56^{BC}$ | $0.46\pm0.08^{B}$ | $655.37\pm54.76^{A}$ | $165.19\pm10.77^{DE}$ | $0.30\pm0.05^{A}$ | $0.80\pm0.02^{A}$ |
| | C+N | $129.80\pm10.32^{AB}$ | $0.43\pm0.03^{B}$ | $388.49\pm45.75^{BC}$ | $263.19\pm8.97^{A}$ | $0.33\pm0.02^{A}$ | $0.59\pm0.03^{B}$ |
| Unfertilized Mixture | C | $111.33\pm32.61^{ABC}$ | $0.31\pm0.10^{B}$ | $434.85\pm27.38^{ABC}$ | $154.35\pm5.55^{E}$ | $0.39\pm0.08^{A}$ | $0.74\pm0.01^{AB}$ |
| | C+N | $122.12\pm13.95^{ABC}$ | $0.57\pm0.16^{B}$ | $326.87\pm59.67^{C}$ | $186.54\pm5.60^{CDE}$ | $0.39\pm0.03^{A}$ | $0.62\pm0.04^{B}$ |
| Fertilized *B. nana* | C | $79.26\pm2.46^{ABC}$ | $0.85\pm0.02^{A}$ | $610.75\pm12.91^{AB}$ | $197.54\pm9.68^{BCDE}$ | $0.29\pm0.02^{A}$ | $0.76\pm0.01^{AB}$ |
| | C+N | $53.03\pm4.86^{C}$ | $1.14\pm0.23^{A}$ | $387.14\pm49.26^{BC}$ | $203.81\pm4.87^{BCD}$ | $0.29\pm0.10^{A}$ | $0.65\pm0.02^{AB}$ |
| FT | | ** | *** | ** | *** | | |
| LT | | | | ** | *** | | ** |
| FT×LT | | ** | | ** | ** | | * |

Values represent the mean±s.e. from laboratory treatment additions of $^{13}$C-glucose (C) and $^{13}$C-glucose and $NH_4NO_3$ (C+N) to non-fertilized soils underlying *B. nana* ($n$=5), *E. vaginatum* ($n$=5), a non-specific (mixture) of vegetation ($n$=4) and 35-yr-fertilization soils underlying *B. nana* ($n$=3). Treatment means that share the same letter (A–D) are not statistically different from each other. $^{13}$C pools of MB-C, DOC, soil and cumulative respiration ($CO_2$) are shown. The level of significance from the two-way ANOVA model including FT, LT and their interaction (FT×LT) is reported as *$P$<0.05, **$P$<0.01 or ***$P$<0.001. [a]Microbial CUE. [b]CSE, proportion of $^{13}$C added.

inputs differ between shrub and graminoid soils[18] but the longer-term effects of enhanced soil nutrient availability on the ecosystem C balance remained unclear. Complementing 35 years of field nutrient manipulations with C and N amendments in the laboratory enabled us to distinguish short- from long-term fertilization effects on microbial CUE and SOC priming and to extrapolate how the strength of stoichiometric linkages among ecosystem components influenced the timing and magnitude of SOC loss and recovery. We suggest that initially (0–20 years of experimentation), when annual litter production included a significant portion of high C:N and polysaccharide-rich graminoid litter (Supplementary Figs. 1 and 2), elevated soil C:N values led to severe N limitation for both plants and microbial decomposers, particularly in the biologically active surface soil (Supplementary Table 3). Nutrient addition to severely N-limited soils allowed microbial communities to invest in enzyme synthesis[53,54] inducing a positive priming cascade that resulted in dramatic, albeit short-term, SOC loss. Over time (20–35 years of experimentation), increases in shrub expansion (facilitated by soil nutrient availability) and the delivery of lower C:N and structurally complex litter inputs belowground alleviated microbial N constraints but intensified labile C limitation (Supplementary Table 3). As shrub inputs reduced microbial decomposition, SOC formation began to exceed SOC loss, gradually rebuilding SOC stocks.

By merging long-term observational data with mechanistic experimentation, we demonstrate how net ecosystem C balance shifts during a strong press disturbance (chronic fertilization). While the fertilization rate used at the Toolik Lake Long-Term Ecological Research site (+10 gN $m^{-2}$ $yr^{-1}$) is far higher than the Arctic will experience under ambient climate change (approximately +2.4 gN $m^{-2}$ $yr^{-1}$ in control plots), the combined pressures of atmospheric deposition, nutrient release from thawing permafrost and warming-induced mineralization necessitates a long-term and mechanistic understanding of tundra resilience to nutrient enrichment. By experimentally accelerating shrub expansion and alleviating ecosystem nutrient constraints we identified three key mechanisms underlying Arctic SOC storage. First, using one of the longest running ecosystem manipulation experiments, we found that SOC losses were ephemeral and depend on shifts in aboveground plant community composition that drive changes in belowground nutrient cycling. Second, we present experimental and observational evidence suggesting that positive priming cascades do not persist long-term, challenging previous findings and a fundamental tenet of next-generation soil C models[16]. Furthermore, our experimental data highlight the need for land surface models to adopt more detailed vegetation trait dynamics and their impacts on ecosystem productivity. Third, we show that SOC responses to press nutrient disturbance depend on stoichiometric constraints and interactions among ecosystem components. As a result, changes in SOC storage cannot be predicted simply by applying a temperature sensitivity factor to active layer SOC decomposition rates[55–57]. Determining whether the short- to long-term mechanistic feedbacks demonstrated in our study are themselves broadly predictable represents a major unmet challenge for experimental and observational studies and highlights the importance of testing ecological theory at longer timescales[30,58,59] and across diverse regions[60]. For instance, although widespread increases in shrub abundance and productivity across the Arctic[36] may generate similar interactive effects among plants, microorganisms and soil biogeochemical cycles, shifts in the SOC balance could differ on the basis of site-specific conditions (for example, differences in initial C/N/P limitation, vegetation cover, N deposition, cryoturbation, hydrology, microbial community composition and so on). Constraining the effect of fine-scale mechanisms on the SOC balance is therefore critical for predicting the magnitude and direction of the Arctic C–climate feedback.

## Online content

Any methods, additional references, Nature Portfolio reporting summaries, source data, extended data, supplementary information, acknowledgements, peer review information; details of author contributions and competing interests; and statements of data and code availability are available at https://doi.org/10.1038/s41558-024-02147-3.

## References

1. Tarnocai, C. et al. Soil organic carbon pools in the northern circumpolar permafrost region. *Global Biogeochem. Cycles* https://doi.org/10.1029/2008GB003327 (2009).
2. Rantanen, M. et al. The Arctic has warmed nearly four times faster than the globe since 1979. *Commun. Earth Environ.* **3**, 168 (2022).
3. Davidson, E. & Janssens, I. Temperature sensitivity of soil carbon decomposition and feedbacks to climate change. *Nature* **440**, 165–173 (2006).
4. Carey, J. C. et al. Temperature response of soil respiration largely unaltered with experimental warming. *Proc. Natl Acad. Sci. USA* **113**, 13797–13802 (2016).
5. Crowther, T. et al. Quantifying global soil carbon losses in response to warming. *Nature* **540**, 104–108 (2016).
6. Hartley, I. P. et al. A potential loss of carbon associated with greater plant growth in the European Arctic. *Nat. Clim. Change* **2**, 875–879 (2012).

7. Mack, M. C., Schuur, E. A., Bret-Harte, M. S., Shaver, G. R. & Chapin, F. S. Ecosystem carbon storage in Arctic tundra reduced by long-term nutrient fertilization. *Nature* **431**, 440–443 (2004).
8. Capek, P. et al. A plant–microbe interaction framework explaining nutrient effects on primary production. *Nat. Ecol. Evol.* **2**, 1588–1596 (2018).
9. Shaver, G., Chapin, F. III & Gartner, B. L. Factors limiting seasonal growth and peak biomass accumulation in *Eriophorum vaginatum* in Alaskan tussock tundra. *J. Ecol.* **74**, 257–278 (1986).
10. LeBauer, D. S. & Treseder, K. K. Nitrogen limitation of net primary productivity in terrestrial ecosystems is globally distributed. *Ecology* **89**, 371–379 (2008).
11. Treseder, K. K. Nitrogen additions and microbial biomass: a meta-analysis of ecosystem studies. *Ecol. Lett.* **11**, 1111–1120 (2008).
12. Schimel, J. P. & Weintraub, M. N. The implications of exoenzyme activity on microbial carbon and nitrogen limitation in soil: a theoretical model. *Soil Biol. Biochem.* **35**, 549–563 (2003).
13. Sistla, S. A., Asao, S. & Schimel, J. P. Detecting microbial N-limitation in tussock tundra soil: implications for Arctic soil organic carbon cycling. *Soil Biol. Biochem.* **55**, 78–84 (2012).
14. Hartley, I. P., Hopkins, D. W., Sommerkorn, M. & Wookey, P. A. The response of organic matter mineralisation to nutrient and substrate additions in sub-arctic soils. *Soil Biol. Biochem.* **42**, 92–100 (2010).
15. Wild, B. et al. Input of easily available organic C and N stimulates microbial decomposition of soil organic matter in Arctic permafrost soil. *Soil Biol. Biochem.* **75**, 143–151 (2014).
16. Keuper, F. et al. Carbon loss from northern circumpolar permafrost soils amplified by rhizosphere priming. *Nat. Geosci.* **13**, 560–565 (2020).
17. Tape, K., Sturm, M. & Racine, C. The evidence for shrub expansion in Northern Alaska and the Pan-Arctic. *Glob. Change Biol.* **12**, 686–702 (2006).
18. Lynch, L. M., Machmuller, M. B., Cotrufo, M. F., Paul, E. A. & Wallenstein, M. D. Tracking the fate of fresh carbon in the Arctic tundra: will shrub expansion alter responses of soil organic matter to warming? *Soil Biol. Biochem.* **120**, 134–144 (2018).
19. Hobbie, S. E. Temperature and plant species control over litter decomposition in Alaskan tundra. *Ecol. Monogr.* **66**, 503–522 (1996).
20. Cornelissen, J. H. et al. Global negative vegetation feedback to climate warming responses of leaf litter decomposition rates in cold biomes. *Ecol. Lett.* **10**, 619–627 (2007).
21. Shaver, G. R. & Chapin, F. S. III Production: biomass relationships and element cycling in contrasting Arctic vegetation types. *Ecol. Monogr.* **61**, 1–31 (1991).
22. Chapin, F. S., Shaver, G. R., Giblin, A. E., Nadelhoffer, K. J. & Laundre, J. A. Responses of Arctic tundra to experimental and observed changes in climate. *Ecology* **76**, 694–711 (1995).
23. Chapin, F. S. et al. The changing global carbon cycle: linking plant–soil carbon dynamics to global consequences. *J. Ecol.* **97**, 840–850 (2009).
24. Todd-Brown, K. E. O. et al. Changes in soil organic carbon storage predicted by Earth system models during the 21st century. *Biogeosciences* **11**, 2341–2356 (2014).
25. Qian, H., Joseph, R. & Zeng, N. Enhanced terrestrial carbon uptake in the northern high latitudes in the 21st century from the coupled carbon cycle climate model intercomparison project model projections. *Glob. Change Biol.* **16**, 641–656 (2010).
26. He, Y. et al. Radiocarbon constraints imply reduced carbon uptake by soils during the 21st century. *Science* **353**, 1419–1424 (2016).
27. Lehmann, J. & Kleber, M. The contentious nature of soil organic matter. *Nature* **528**, 60–68 (2015).
28. Bouskill, N. J., Riley, W. J., Zhu, Q., Mekonnen, Z. A. & Grant, R. F. Alaskan carbon–climate feedbacks will be weaker than inferred from short-term experiments. *Nat. Commun.* **11**, 5798 (2020).
29. Melillo, J. et al. Soil warming and carbon-cycle feedbacks to the climate system. *Science* **298**, 2173 (2002).
30. Reich, P. B., Hobbie, S. E., Lee, T. D. & Pastore, M. A. Unexpected reversal of C3 versus C4 grass response to elevated $CO_2$ during a 20-year field experiment. *Science* **360**, 317–320 (2018).
31. Bockheim, J., Hinkel, K. & Nelson, F. Predicting carbon storage in tundra soils of arctic Alaska. *Soil Sci. Soc. Am. J.* **67**, 948–950 (2003).
32. Michaelson, G. J., Ping, C. & Kimble, J. Carbon storage and distribution in tundra soils of Arctic Alaska, USA. *Arct. Alp. Res.* **28**, 414–424 (1996).
33. Peng, X. et al. Active layer thickness and permafrost area projections for the 21st century. *Earth's Future* **11**, e2023EF003573 (2023).
34. Shaver, G. R. et al. Species composition interacts with fertilizer to control long-term change in tundra productivity. *Ecology* **82**, 3163–3181 (2001).
35. Sturm, M. et al. Winter biological processes could help convert Arctic tundra to shrubland. *Bioscience* **55**, 17–26 (2005).
36. Heijmans, M. M. et al. Tundra vegetation change and impacts on permafrost. *Nat. Rev. Earth Environ.* **3**, 68–84 (2022).
37. Gagnon, M., Domine, F. & Boudreau, S. The carbon sink due to shrub growth on Arctic tundra: a case study in a carbon-poor soil in eastern Canada. *Environ. Res. Commun.* **1**, 091001 (2019).
38. Ackerman, D., Millet, D. B. & Chen, X. Global estimates of inorganic nitrogen deposition across four decades. *Global Biogeochem. Cycles* **33**, 100–107 (2019).
39. Bobbink, R. et al. Global assessment of nitrogen deposition effects on terrestrial plant diversity: a synthesis. *Ecol. Appl.* **20**, 30–59 (2010).
40. Hobara, S. et al. Nitrogen fixation in surface soils and vegetation in an Arctic tundra watershed: a key source of atmospheric nitrogen. *Arct. Antarct. Alp. Res.* **38**, 363–372 (2006).
41. Sistla, S. A. et al. Long-term warming restructures Arctic tundra without changing net soil carbon storage. *Nature* **497**, 615–618 (2013).
42. Bret-Harte, M. S. et al. Developmental plasticity allows *Betula nana* to dominate tundra subjected to an altered environment. *Ecology* **82**, 18–32 (2001).
43. DeMarco, J., Mack, M. C. & Bret-Harte, M. S. Effects of Arctic shrub expansion on biophysical vs. biogeochemical drivers of litter decomposition. *Ecology* **95**, 1861–1875 (2014).
44. McCarthy, M. & Enquist, B. Consistency between an allometric approach and optimal partitioning theory in global patterns of plant biomass allocation. *Funct. Ecol.* **21**, 713-720 (2007).
45. Bloom, A. J., Chapin, F. S. & Mooney, H. A. Resource limitation in plants—an economic analogy. *Annu. Rev. Ecol. Syst.* **16**, 363–392 (1985).
46. Sullivan, P. F. et al. Climate and species affect fine root production with long-term fertilization in acidic tussock tundra near Toolik Lake, Alaska. *Oecologia* **153**, 643–652 (2007).
47. Iversen, C. M. et al. The unseen iceberg: plant roots in Arctic tundra. *New Phytol.* **205**, 34–58 (2015).
48. Tao, F. et al. Microbial carbon use efficiency promotes global soil carbon storage. *Nature* **618**, 981–985 (2023).
49. Dijkstra, P. et al. High carbon use efficiency in soil microbial communities is related to balanced growth, not storage compound synthesis. *Soil Biol. Biochem.* **89**, 35–43 (2015).
50. McLaren, J. R. & Buckeridge, K. M. Decoupled above-and belowground responses to multi-decadal nitrogen and phosphorus amendments in two tundra ecosystems. *Ecosphere* **10**, e02735 (2019).
51. Keller, K., Blum, J. D. & Kling, G. W. Geochemistry of soils and streams on surfaces of varying ages in arctic Alaska. *Arct. Antarct. Alp. Res.* **39**, 84–98 (2007).

52. Mörsdorf, M. A. et al. Deepened winter snow significantly influences the availability and forms of nitrogen taken up by plants in High Arctic tundra. *Soil Biol. Biochem.* **135**, 222–234 (2019).
53. Koyama, A., Wallenstein, M. D., Simpson, R. T. & Moore, J. C. Carbon-degrading enzyme activities stimulated by increased nutrient availability in Arctic tundra soils. *PLoS ONE* **8**, e77212 (2013).
54. Wallenstein, M. D., Mcmahon, S. K. & Schimel, J. P. Seasonal variation in enzyme activities and temperature sensitivities in Arctic tundra soils. *Glob. Change Biol.* **15**, 1631–1639 (2009).
55. Mishra, U. et al. Empirical estimates to reduce modeling uncertainties of soil organic carbon in permafrost regions: a review of recent progress and remaining challenges. *Environ. Res. Lett.* **8**, 035020 (2013).
56. Wieder, W. R., Sulman, B. N., Hartman, M. D., Koven, C. D. & Bradford, M. A. Arctic soil governs whether climate change drives global losses or gains in soil carbon. *Geophys. Res. Lett.* **46**, 14486–14495 (2019).
57. Huntzinger, D. et al. Evaluation of simulated soil carbon dynamics in Arctic-Boreal ecosystems. *Environ. Res. Lett.* **15**, 025005 (2020).
58. Melillo, J. M. et al. Soil warming, carbon-nitrogen interactions and forest carbon budgets. *Proc. Natl Acad. Sci. USA* **108**, 9508–9512 (2011).
59. Slavik, K. et al. Long-term responses of the Kuparuk River ecosystem to phosphorus fertilization. *Ecology* **85**, 939–954 (2004).
60. Parker, T. C. et al. Shrub expansion in the Arctic may induce large-scale carbon losses due to changes in plant–soil interactions. *Plant Soil* **463**, 643–651 (2021).

## Methods

### Site description and experimental design

In late July 2015, we sampled soils in MAT near Toolik Lake Field Station, on the north slope of the Brooks Range in northern Alaska (68° 38′ N, 149° 34′ W, elevation 760 m). The two dominant species in the vegetation at this site are *B. nana*, a dwarf birch, and *E. vaginatum*, a tussock-forming sedge. The soil in this region is classified as a histic pergelic cryaquept[7]. The mean annual temperature is −8 °C, with average January temperature near −23 °C and July temperature near 11 °C; and mean annual precipitation is 316 mm (ref. 61).

In 1981, a fertilization experiment was established at the site including four replicate blocks of 5 × 20 $m^2$ plots[22]. The randomized split plot experimental design included one fertilized and one unfertilized control plot (5 × 20 $m^2$) per block. Since then, fertilization plots have received 10 gN $m^{-2}$ as $NH_4NO_3$ and 5 gP $m^{-2}$ as superphosphate ($P_2O_5$) each spring immediately following snowmelt.

### Soil sampling and analyses

Sampling after 35 years of fertilizer treatment was completed in 2015 on the same plots using the same random sampling methods and replication as in the 20th year of experimentation[7]. We sampled soils at five randomly chosen points along a 20 m transect in each 5 × 20 $m^2$ plot (two treatments × five quadrats per block × four replicate blocks = 40 samples). We used a serrated knife to cut out and remove soil monoliths, which were immediately transferred to the laboratory for further subsampling. The first subsample was further separated into litter, upper organic (0–5 cm), lower organic (>5 cm) and mineral (down to thaw depth) soil layers and used for analysis of bulk C and N content. The second subsample, divided into the same upper organic, lower organic and mineral layers, was used to determine bulk density after subtracting rock, root and stem volume and mass from soil volume and mass.

In addition to these randomly distributed samples (which were topped by a moist tussock tundra vegetation including sedge tussocks, mosses and evergreen and deciduous shrubs[22,35]), we also collected organic soils beneath several individual *B. nana* and *E. vaginatum* plants directly adjacent to control plots to minimize disturbance inside the historic plots. To ensure we collected *E. vaginatum*-conditioned soils alone, we carefully removed all dead plant material from the soil surface and excluded all aerial portions of the tussock. Soil samples were homogenized and composited according to their respective aboveground plant functional type (tussock graminoid versus woody deciduous shrub) before analysis.

Soil monoliths were separated by soil layer into additional subsamples for microbial biomass and extractable C and N (fresh soil), laboratory incubation (soil stored at −20 °C) and C and N stocks (dried at 60 °C). As in previous harvests of this experiment[7,22,34], plant materials including litter, roots, belowground stems and rhizomes were hand-picked from individual quadrat samples and composited by block ($n$ = 4). Soil samples were kept separated by quadrat for all analyses, except the laboratory incubation where we used composited samples. Plant and soil samples were dried at 60 °C and weighed, ground to a fine powder and analysed for C and N content on a Carlo Erba NA 1500 elemental analyser (CE Instruments).

Microbial biomass and extractable C and N were measured on fresh soil following a modified[62] chloroform fumigation–extraction method[63]. To extract microbial biomass, we evenly distributed 4 ml of ethanol-free chloroform over 10 g of fresh soil subsamples and incubated them for 24 h with a stoppered 250 ml Erlenmeyer flask. Following incubation, we vented the chloroform samples under a fume hood for 30 min and extracted unfumigated and fumigated soil subsamples (10 g) and soil-free blanks with 50 ml of 0.5 M $K_2SO_4$. Soil solutions were agitated on an orbital shaker for 1 h, then filtered through no. 1 Whatman paper and analysed for DOC and total dissolved N (TDN) on a Shimadzu TOC-Vcpn total organic C analyser with a total N module (Shimadzu Scientific Instruments). DOC/TDN was obtained from unfumigated soils and extractable microbial biomass was calculated as the difference between paired fumigated and unfumigated subsamples. No correction factors ($k_{eC}$, $k_{eN}$) were applied, as they have not been determined for these soils[53]. We measured extractable ammonium, nitrate and phosphate on unfumigated extracts using colorimetric microplate assays[64–66].

### Isotope-tracing experiment

Homogenized, root-free, field-moist soil (50 g) samples from field plots (long-term fertilized and long-term control) and unfertilized soils collected adjacent to control blocks from underneath *B. nana* or *E. vaginatum* plants were split into glass Mason jars which received one of three laboratory treatments: (1) water-only control, (2) $^{13}$C-enriched glucose or (3) $^{13}$C-enriched glucose + $NH_4NO_3$ solution. Before treatment addition, soils were brought to 60% soil moisture, measured as gravimetric water content. We incubated the jars at 10 °C for 1 week to equilibrate before measurements. Treatment solutions were added dropwise as a 4 ml aqueous solution to each soil and C and N mixtures consisted of 700 µgC per g of dry soil (~0.2% of total soil C) of 10 at% $^{13}$C-glucose C (a common root exudate) and 645 µgN per g of soil (~6% of total soil N) in the form of $NH_4NO_3$. We estimated that the amount of N added was six to 12 times greater than microbial demand (assuming N biomass requirements are 2–4% of the total C respired, 20–40% of the respired C was allocated to microbial biomass C and an average microbial biomass C:N of 10)[13,18]. Five replicates per treatment were used for both *B. nana* and *E. vaginatum* soils ($N_{B.\,nana}$ = five replicates × three treatments = 15 jars; $N_{E.\,vag}$ = five replicates × three treatments = 15 jars). The long-term fertilization field experimental design (blocks) was used for incubation replication but one fertilized plot was excluded from analysis due to low sample size ($N_{control}$ = 4 replicates × three treatments = 12 jars; $N_{fert}$ = three replicates × three treatments = nine jars). Mason jars were capped with an air-tight lid modified with sampling ports used for gas sampling. We incubated all soils at 10 °C for 25 d, which is within the 10–20 °C range of soil temperatures during the growing season[67]. We kept soil moisture constant by measuring the mass of each incubation jar at every soil respiration sampling point and adding water as necessary to maintain 60% gravimetric water content.

### Soil respiration

We sampled the headspace from all jars for total $CO_2$ and $^{13}$C-$CO_2$ concentrations at nine time points after the treatment additions: 3, 6, 24 and 48 h and 5, 8, 11, 14 and 25 d. Total $CO_2$ concentrations were measured immediately with a Licor 6252 gas analyser (Licor) and an additional sample was placed in an evacuated vial for $^{13}$C-$CO_2$ isotopic analysis on a VG Optima GC-IRMS (Isoprime). Licor infrared gas analysers are less sensitive to $^{13}CO_2$ than to $^{12}CO_2$ (for example, they underestimate $CO_2$ concentrations by up to 66%). Using this percentage, we calculated the unbiased $CO_2$ concentration accounting for the undetected $^{13}$C-$CO_2$ at each time point (that is, what would have been measured if 100% of the $^{13}CO_2$ molecules were detected) to correct cumulative $CO_2$ respiration. Because corrected values varied by <5% from measured values and statistical trends among treatments were identical, we report the measured values.

### Soil analyses

After 25 d, we harvested the soil to determine total soil C, N, DOC, TDN (organic and inorganic) and microbial biomass C and N. We measured $^{13}$C in bulk soil, dissolved and microbial pools to determine the fate of $^{13}$C-glucose. Soil subsamples (2–5 g) were dried at 60 °C, ground to a fine powder and analysed for total C, N and $\delta^{13}$C using a Carlo Erba NA 1500 elemental analyser (CE Instruments) coupled to a VG Isochrom continuous flow isotope ratio mass spectrometer (Isoprime). Using fresh soil, we measured microbial biomass and extractable C and N using the method described above, except we used a weaker salt solution (0.05 M $K_2SO_4$) to prevent instrumentation problems during

isotopic analysis on dried salt extracts. To quantify C derived from $^{13}$C-glucose in dissolved C and microbial biomass pools, we lyophilized extracts using a FreeZone 6 Liter console freeze dry system (Labcono) and analysed lyophilized subsamples for $\delta^{13}$C using a Carlo Erba NA 1500 elemental analyser (CE Instruments) coupled to a VG Isochrom continuous flow isotope ratio mass spectrometer (Isoprime).

### Changes in soil C and N across time

Changes in total soil N stocks (including roots) were calculated as:

$$\Delta N_{\text{treatment}} = \Delta N_{\text{control}} + \Delta N_{\text{fertilizer input}} + \Delta N_{\text{unexplained}} \quad (1)$$

where

$$\Delta N_{\text{treatment}} = N_{\text{Trt2015}} - N_{\text{Trt2000}}$$

$$\Delta N_{\text{control}} = N_{\text{Ctrl2015}} - N_{\text{Ctrl2000}}$$

Here $\Delta N_{\text{control}}$ captures changes in soil biogeochemistry in the absence of exogenous fertilizer input and is estimated using the change in soil C and N of control plots across time, and

$$\Delta N_{\text{fertilizer input}} = 10\ \text{gN m}^{-2}\ \text{yr}^{-1} \times 15\ \text{yr} = 150\ \text{gN m}^{-2}$$

where net change in soil N between 2000 and 2015 is calculated as:

$$365\ \text{gN m}^{-2} = 36\ \text{gN m}^{-2} + 150\ \text{gN m}^{-2} + x = +179\ \text{gN m}^{-2}$$

Similarly, changes in total soil C stocks between 2000 and 2015 (including roots) were calculated as:

$$\Delta C_{\text{treatment}} = \Delta C_{\text{control}} + \Delta C_{\text{fertilizer input}} + \Delta C_{\text{unexplained}} \quad (2)$$

where

$$\Delta C_{\text{treatment}} = C_{\text{Trt2015}} - C_{\text{Trt2000}}$$

$$\Delta C_{\text{control}} = C_{\text{Ctrl2015}} - C_{\text{Ctrl2000}}$$

$$\Delta C_{\text{fertilizer input}} = 0\ \text{gC m}^{-2}\ \text{yr}^{-1} \times 15\ \text{yr} = 0\ \text{gC m}^{-2}$$

Net change in soil C between 2000 and 2015 is calculated as:

$$7,943\ \text{gC m}^{-2} = 943\ \text{gC m}^{-2} + 0\ \text{gC m}^{-2} + x = +7,000\ \text{gC m}^{-2}$$

### Estimates of NPP between 20th and 35th year of experimentation

We used the average (per treatment) of measured NPP in 2000 and 2015 to estimate NPP inputs over 15 years in both control and fertilized plots. Measured NPP (mean ± s.e.) in 20 yr control = 521.31 ± 205.30; 20 yr fertilized = 743.47 ± 89.08; 35 yr control 678.44 ± 88.88; and 35 yr fertilized = 763.17 ± 141.51.

### Mass balance model

A mass balance equation was used to determine the $\delta^{13}$C value of microbial biomass ($\delta^{13}C_{MB}$):

$$\Delta^{13}C_{\text{MB}} = \delta^{13}C_{\text{fum}} \times C_{\text{fum}} - \delta^{13}C_{\text{nf}} \times C_{\text{nf}}/(C_{\text{fum}} - C_{\text{nf}}), \quad (3)$$

where $\delta^{13}C_{\text{fum}}$ and $\delta^{13}C_{\text{nf}}$ are the $\delta^{13}$C values of the fumigated and non-fumigated samples, respectively, and $C_{\text{fum}}$ and $C_{\text{nf}}$ are the concentrations of C in the fumigated and non-fumigated $K_2SO_4$ samples, respectively[68].

### Mixing model

A two-pool isotopic mixing model[69,70] was next applied to determine the incorporation or loss of the $^{13}$C-glucose in microbial biomass (using the adjusted $\delta^{13}C_{\text{MB}}$ value calculated above), soil and $CO_2$:

$$f_X = \frac{\delta_S - \delta_C}{\delta_g - \delta_C} \quad (4)$$

where $f_X$ is the amount of glucose C in the pool of interest ($X$, for example, MB, soil or $CO_2$), $\delta_S$ is the $\delta^{13}$C of glucose-amended sample (S), $\delta_C$ is the $\delta^{13}$C of the water-only control sample (C), $\delta_g$ is the $\delta^{13}$C of the glucose added (g). A positive priming effect (after C and/or N additions) was defined as greater native soil C respiration than control (water-only addition)[71]. We defined microbial CUE as the partitioning of $^{13}$C-enriched glucose between growth and respiration[72]:

$$\text{CUE} = {}^{13}\text{MB}/\left({}^{13}\text{MB} + {}^{13}\text{CO}_2\right), \quad (5)$$

where $^{13}$MB represents $^{13}$C-enriched glucose assimilated in microbial biomass (gC per g of soil) and $^{13}CO_2$ represents the fraction of $^{13}$C-enriched glucose converted to $CO_2$ (gC per g of soil). We similarly define C stabilization efficiency (CSE) as the partitioning of $^{13}$C-enriched glucose between bulk soils ($^{13}C_{\text{bulk soil}}$) and respiration ($^{13}CO_2$):

$$\text{CSE} = {}^{13}\text{C}_{\text{bulk soil}}/\left({}^{13}\text{C}_{\text{bulk soil}} + {}^{13}\text{CO}_2\right). \quad (6)$$

Isotope recovery efficiencies are reported in Supplementary Table 2.

### Plant and SOM chemistry—py-MBMS

Plant and SOM chemistry was measured with pyrolysis molecular beam mass spectrometry (py-MBMS)[73] using 20–200 mg of soil and 10–50 mg of plant sample. Each individual sample was analysed in duplicate. Soil samples were oven dried at 60 °C before analysis and pyrolysed at 550 °C in a reactor consisting of a quartz tube (2.5 cm inside diameter) with 5 l min$^{-1}$ helium flow until the total ion intensity returned to background levels (~3 min). The quartz reactor was connected to the sampling orifice of the MBMS. An Extrel TM model TQMS C50 system was used for the analysis of pyrolysis vapours. Residence time of the vapours was short enough to minimize secondary reactions in the quartz reactor[74,75]. Mass spectral data from $m/z$ 20 to 550 were acquired on a Teknivent Vector 2TM data acquisition system using 22 eV electron impact ionization but only $m/z$ 58–550 were retained for analysis. Repetitive scans (one 480 a.m.u. scan s$^{-1}$) were recorded during the evolution of a pyrolysis wave from each soil sample and then averaged across all scans. For all spectra, a blank spectral signal was subtracted before data analysis. Compound category summaries were calculated using published compound categories[76].

### Plant and SOM chemistry—Fourier-transform infrared spectroscopy

Dried and ground plant and soil samples were scanned from 4,000 to 400 cm$^{-1}$ in diffuse reflectance mode using a Digilab FTS 7000 infrared spectrometer (Varian) with a deuterated triglycine sulfate detector, a KBr beam splitter and a Pike AutoDIFF diffuse reflectance autosampler (Pike Technologies). KBr was used as background. Data were recorded as pseudo absorbance (log [1/Reflectance]), with 4 cm$^{-1}$ resolution and 64 scans co-added per spectrum. Spectral averages and spectral subtractions were performed using GRAMS AI v.9.1 software (Thermo Fisher). Principal components analysis of the spectral data was performed with the Unscrambler software v.10.4 (CAMO). Spectral data were mean-centred before the analysis.

### Statistics

To determine the effect of long-term field fertilization and vegetation type on the fate of $^{13}$C-glucose, we performed a two-way analysis

of variance (ANOVA) (JMP 17.0, SAS Institute). The ANOVA included cumulative $^{13}C$ incorporation into all measured pools (for example, soil, microbial biomass, DOC and respiration) as response variables with the following factors: field treatment (fertilized and unfertilized), laboratory treatment (glucose, glucose + $NH_4NO_3$ and control) and the two-way interaction of field × laboratory treatment (Table 2). We did not find a significant effect of block when including it as a random effect in the model, so we opted to leave it out of the final statistical model. A similar two-way ANOVA was performed for non-glucose pools. Soil biogeochemical measurements from long-term experimental plots (Table 1) were also statistically analysed using a two-way ANOVA with soil layer, field treatment (fertilized and unfertilized) and their interaction. Tukey's honestly significant differences (HSD) and Student's *t*-test post hoc analysis was used for comparison of the main effects and their interactions. For all statistical analyses, data were tested for normality and log transformed if necessary to acquire normal distribution of residuals.

### Reporting summary

Further information on research design is available in the Nature Portfolio Reporting Summary linked to this article.

## Data availability

Data generated during the study can be found within the NSF Arctic data centre (https://arcticdata.io/catalog/view/doi:10.18739/A2833N104). All samples were collected in accordance with relevant permits and local laws. Source data are provided with this paper.

## References


61. *NEON Site Level Plot Summary, Toolik Lake (TOOL)* (NSF, 2019); www.neonscience.org/field-sites/tool
62. Weintraub, M. N., Scott-Denton, L. E., Schmidt, S. K. & Monson, R. K. The effects of tree rhizodeposition on soil exoenzyme activity, dissolved organic carbon and nutrient availability in a subalpine forest ecosystem. *Oecologia* **154**, 327–338 (2007).
63. Brookes, P., Landman, A., Pruden, G. & Jenkinson, D. Chloroform fumigation and the release of soil nitrogen: a rapid direct extraction method to measure microbial biomass nitrogen in soil. *Soil Biol. Biochem.* **17**, 837–842 (1985).
64. Rhine, E., Mulvaney, R., Pratt, E. & Sims, G. Improving the Berthelot reaction for determining ammonium in soil extracts and water. *Soil Sci. Soc. Am. J.* **62**, 473–480 (1998).
65. Doane, T. A. & Horwáth, W. R. Spectrophotometric determination of nitrate with a single reagent. *Anal. Lett.* **36**, 2713–2722 (2003).
66. D'Angelo, E., Crutchfield, J. & Vandiviere, M. Rapid, sensitive, microscale determination of phosphate in water and soil. *J. Environ. Qual.* **30**, 2206–2209 (2001).
67. Shaver, G. R. et al. Carbon turnover in Alaskan tundra soils: effects of organic matter quality, temperature, moisture and fertilizer. *J. Ecol.* **94**, 740–753 (2006).
68. Werth, M. & Kuzyakov, Y. Root-derived carbon in soil respiration and microbial biomass determined by $^{14}C$ and $^{13}C$. *Soil Biol. Biochem.* **40**, 625–637 (2008).
69. Balesdent, J., Wagner, G. & Mariotti, A. Soil organic matter turnover in long-term field experiments as revealed by carbon-13 natural abundance. *Soil Sci. Soc. Am. J.* **52**, 118–124 (1988).
70. Rubino, M. et al. An isotopic method for testing the influence of leaf litter quality on carbon fluxes during decomposition. *Oecologia* **154**, 155–166 (2007).
71. Kuzyakov, Y. Priming effects: interactions between living and dead organic matter. *Soil Biol. Biochem.* **42**, 1363–1371 (2010).
72. Manzoni, S., Taylor, P., Richter, A., Porporato, A. & Ågren, G. I. Environmental and stoichiometric controls on microbial carbon-use efficiency in soils. *New Phytol.* **196**, 79–91 (2012).
73. Magrini, K., Evans, R., Hoover, C., Elam, C. & Davis, M. Use of pyrolysis molecular beam mass spectrometry (py-MBMS) to characterize forest soil carbon: method and preliminary results. *Environ. Pollut.* **116**, S255–S268 (2002).
74. Evans, R. J. & Milne, T. A. Molecular characterization of the pyrolysis of biomass. *Energy Fuels* **1**, 123–137 (1987).
75. Plante, A. F., Magrini-Bair, K., Vigil, M. & Paul, E. A. Pyrolysis molecular beam mass spectrometry to characterize soil organic matter composition in chemically isolated fractions from differing land uses. *Biogeochemistry* **92**, 145–161 (2009).
76. Haddix, M. L. et al. Progressing towards more quantitative analytical pyrolysis of soil organic matter using molecular beam mass spectroscopy of whole soils and added standards. *Geoderma* **283**, 88–100 (2016).


## Acknowledgements

We thank J. Laundre for his assistance and maintenance of long-term experiment plots, R. Simpson and J. Moore for help with field sampling and the Toolik Field Station staff for their logistical support. This work was supported by a National Science Foundation CAREER award (grant no. 1255228) to M.D.W. and a Department of Energy Terrestrial and Ecosystem Science programme award (grant no. DE-SC0010568) to M.D.W. The long-term experiments have been maintained by the Toolik LTER project (DEB-1637459 and earlier awards).

## Author contributions

M.B.M., L.M.L. and J.R.M. all contributed to field sample collection, led by G.R.S. and L.G. M.B.M, L.M.L. and S.L.M. performed measurements from isotope-tracing laboratory incubation. M.N.W. performed measurements of soil nutrients from long-term experimental plots. F.C. performed Fourier-transform infrared spectroscopy and M.L.H. performed py-MBMS measurements for soil and plant chemistry. M.B.M. coordinated the project and led paper preparation and data analyses. G.R.S., M.N.W., E.A.P., M.F.C. and M.D.W. contributed to data interpretation. All authors contributed to writing the paper.

## Competing interests

The authors declare no competing interests.

## Additional information

**Supplementary information** The online version contains supplementary material available at https://doi.org/10.1038/s41558-024-02147-3.

**Correspondence and requests for materials** should be addressed to Megan B. Machmuller.

**Peer review information** *Nature Climate Change* thanks Birgit Wild and the other, anonymous, reviewer(s) for their contribution to the peer review of this work.

nature portfolio

Corresponding author(s): Megan Machmuller

Last updated by author(s): Jul 4, 2023

# Reporting Summary

Nature Portfolio wishes to improve the reproducibility of the work that we publish. This form provides structure for consistency and transparency in reporting. For further information on Nature Portfolio policies, see our Editorial Policies and the Editorial Policy Checklist.

## Statistics

For all statistical analyses, confirm that the following items are present in the figure legend, table legend, main text, or Methods section.

| n/a | Confirmed | |
|---|---|---|
| ☐ | ☒ | The exact sample size (*n*) for each experimental group/condition, given as a discrete number and unit of measurement |
| ☐ | ☒ | A statement on whether measurements were taken from distinct samples or whether the same sample was measured repeatedly |
| ☐ | ☒ | The statistical test(s) used AND whether they are one- or two-sided<br>*Only common tests should be described solely by name; describe more complex techniques in the Methods section.* |
| ☐ | ☒ | A description of all covariates tested |
| ☐ | ☒ | A description of any assumptions or corrections, such as tests of normality and adjustment for multiple comparisons |
| ☐ | ☒ | A full description of the statistical parameters including central tendency (e.g. means) or other basic estimates (e.g. regression coefficient) AND variation (e.g. standard deviation) or associated estimates of uncertainty (e.g. confidence intervals) |
| ☐ | ☒ | For null hypothesis testing, the test statistic (e.g. *F*, *t*, *r*) with confidence intervals, effect sizes, degrees of freedom and *P* value noted<br>*Give P values as exact values whenever suitable.* |
| ☒ | ☐ | For Bayesian analysis, information on the choice of priors and Markov chain Monte Carlo settings |
| ☒ | ☐ | For hierarchical and complex designs, identification of the appropriate level for tests and full reporting of outcomes |
| ☒ | ☐ | Estimates of effect sizes (e.g. Cohen's *d*, Pearson's *r*), indicating how they were calculated |

*Our web collection on statistics for biologists contains articles on many of the points above.*

## Software and code

Policy information about availability of computer code

| | |
|---|---|
| Data collection | no software used |
| Data analysis | JMP software 17.0 (SAS Corp, Grams AI version 9.1Thermo Fisher, Woburn, MA), Unscrambler software version 10.4 (CAMO, Norway). |

For manuscripts utilizing custom algorithms or software that are central to the research but not yet described in published literature, software must be made available to editors and reviewers. We strongly encourage code deposition in a community repository (e.g. GitHub). See the Nature Portfolio guidelines for submitting code & software for further information.

## Data

Policy information about availability of data

All manuscripts must include a data availability statement. This statement should provide the following information, where applicable:

- Accession codes, unique identifiers, or web links for publicly available datasets
- A description of any restrictions on data availability
- For clinical datasets or third party data, please ensure that the statement adheres to our policy

Data generated during the study can be found within the NSF Arctic data center (https://arcticdata.io/catalog/data). Source data for figures displayed in manuscript available in Supplementary Information. All samples were collected in accordance with relevant permits and local laws.

## Human research participants

Policy information about studies involving human research participants and Sex and Gender in Research.

| | |
|---|---|
| Reporting on sex and gender | No data collected |
| Population characteristics | No data collected |
| Recruitment | Not applicable |
| Ethics oversight | Not abblicable |

Note that full information on the approval of the study protocol must also be provided in the manuscript.

# Field-specific reporting

Please select the one below that is the best fit for your research. If you are not sure, read the appropriate sections before making your selection.

☐ Life sciences ☐ Behavioural & social sciences ☒ Ecological, evolutionary & environmental sciences

For a reference copy of the document with all sections, see nature.com/documents/nr-reporting-summary-flat.pdf

# Ecological, evolutionary & environmental sciences study design

All studies must disclose on these points even when the disclosure is negative.

| | |
|---|---|
| Study description | In 1981, a fertilization experiment was established at the site, as detailed elsewhere22. Since then, fertilization plots have received 10 g m-2 N as NH4NO3 and 5 g m-2 P as superphosphate (P2O5) each spring immediately following snowmelt. The split plot experimental design consists of four replicate blocks, with one fertilized and one unfertilized control plot (5 x 20 m) per block. |
| Research sample | After 35 years of fertilization, we sampled soils in five 10 x 40 cm quadrats that were randomly arrayed along a 20 m transect in each block. Other data used from Mack et al. Ecosystem carbon storage in arctic tundra reduced by long-term nutrient fertilization. Nature 431, 440-443 (2004). |
| Sampling strategy | We used a knife to saw and manually remove soil monoliths, which we separated in the field, into litter, upper organic (0-5 cm), lower organic (> 5 cm), and mineral (down to thaw depth) horizons. In each block, we also sampled two 10 x 10 cm monoliths that were used to determine bulk density, after subtracting rock, root, stem volume and mass from soil volume and mass. Sampling strategy was based on previous sampling performed in these plots (Mack et al 2004, Nature) for consistency and adequate comparison. |
| Data collection | M.B.M., L.L., and J.R.M all contributed to field sample collection, led by G.R.S. and L.G. M.B.M, L.L., and S.L.M. performed measurements from isotope-tracing laboratory incubation. M.N.W. performed measurements of soil nutrients from long-term experimental plots. F.C. performed FTIR and M.L.H. performed pyMBMS measurements for soil and plant chemistry. |
| Timing and spatial scale | After 35 years of fertilization, we sampled soils in five 10 x 40 cm quadrats that were randomly arrayed along a 20 m transect in each block. We used a knife to saw and manually remove soil monoliths, which we separated in the field, into litter, upper organic (0-5 cm), lower organic (> 5 cm), and mineral (down to thaw depth) horizons. In each block, we also sampled two 10 x 10 cm monoliths that were used to determine bulk density, after subtracting rock, root, stem volume and mass from soil volume and mass. |
| Data exclusions | The long-term fertilization field experimental design (blocks) was used for incubation replication, but one fertilized plot was excluded from analysis due to low sample size (NControl = 12, NFert = 9). |
| Reproducibility | We sampled soils in experimental plots with the same method used previously (see Mack et al 2004, Nature) to assure adequate comparison of findings. |
| Randomization | Soil samples were taken at random locations within each experimental plot before composited. Composited samples were analyzed for soil carbon and nitrogen stocks. |
| Blinding | Blinding was not relevant to this study |

Did the study involve field work? ☒ Yes ☐ No

## Field work, collection and transport

| | |
|---|---|
| Field conditions | In late July 2015, we sampled soils in moist acidic tundra near Toolik Lake Field Station, on the north slope of the Brooks Range in northern Alaska (68°38′ N, 149°34′ W, elevation 760 m). The two dominant vegetation types characterizing this site are Betula nana, a dwarf birch, and Eriophorum vaginatum, a tussock forming sedge. The soil in this region is classified as a histic pergelic cryaquept. The mean annual temperature is -8 °C, with average January temperature near -23 °C and July temperature near 11 °C (Supplementary Fig. 4); mean annual precipitation is 316 mm. |
| Location | Toolik Lake Field Station, on the north slope of the Brooks Range in northern Alaska (68°38′ N, 149°34′ W, elevation 760 m) |
| Access & import/export | Sampling permits issued by the BLM and permission granted by the Toolik Lake Arctic LTER to sample long-term experimental plots. |
| Disturbance | Core sampling and disturbance area was flagged and documented, records of disturbance and samples stored within the Arctic LTER. |

# Reporting for specific materials, systems and methods

We require information from authors about some types of materials, experimental systems and methods used in many studies. Here, indicate whether each material, system or method listed is relevant to your study. If you are not sure if a list item applies to your research, read the appropriate section before selecting a response.

### Materials & experimental systems

| n/a | Involved in the study |
|---|---|
| ☒ | ☐ Antibodies |
| ☒ | ☐ Eukaryotic cell lines |
| ☒ | ☐ Palaeontology and archaeology |
| ☒ | ☐ Animals and other organisms |
| ☒ | ☐ Clinical data |
| ☒ | ☐ Dual use research of concern |

### Methods

| n/a | Involved in the study |
|---|---|
| ☒ | ☐ ChIP-seq |
| ☒ | ☐ Flow cytometry |
| ☒ | ☐ MRI-based neuroimaging |